APPLIED PHYSICS LETTERS **93**, 071102 (2008)

Simultaneous interfacial misfit array formation and antiphase domain suppression on miscut silicon substrate

S. H. Huang,[1,2,a)] G. Balakrishnan,[1] A. Khoshakhlagh,[1] L. R. Dawson,[1] and D. L. Huffaker[1,3]

[1]*Center for High Technology Materials, University of New Mexico, Albuquerque, New Mexico 87106, USA*
[2]*TEM Laboratory, Department of Earth and Planetary Sciences, University of New Mexico, Albuquerque, New Mexico 87131, USA*
[3]*California Nano Systems Institute and Department of Electrical Engineering, University of California Los Angeles, California 90095, USA*

(Received 23 June 2008; accepted 26 July 2008; published online 18 August 2008)

The authors describe simultaneous interfacial misfit (IMF) array formation along with antiphase domain (APD) suppression in highly mismatched ($\Delta a_0/a_0=13\%$) AlSb grown on a 5° miscut Si (001) substrate. Strain energy from the AlSb/Si heterojunction is accommodated by a self-assembled two-dimensional array of pure 90° dislocations confined to the interface. The 13% lattice mismatch establishes the AlSb/Si IMF period of ~3.46 nm. This IMF spacing is well matched to the step length of the 5° miscut Si (001) substrate. Furthermore, the miscut substrate geometry suppresses APD formation due to the double step height. The resulting bulk material has both very low defect density ($\sim 7\times10^5/\text{cm}^2$) and very low APD density ($\sim 10^3/\text{cm}^2$) confirmed by transmission electron microscope images. This material is expected to be desirable for electronic III-V devices on Si substrates. © *2008 American Institute of Physics*. [DOI: 10.1063/1.2970997]

The monolithic growth of III-V materials on Si offers several desirable features such as efficient use of the integrating platform and reduced processing complexity.[1–4] However, mismatch in lattice constant, thermal expansion coefficient, and process temperature hinder a stable and repeatable production process.[5] Recently, a special growth technique involving 90° interfacial misfit (IMF) dislocations formed using the III-Sb material systems has been demonstrated by our group.[6–8] The IMF relieves strain from extremely mismatched material systems immediately at the interface and results in very low defect density ($<10^6/\text{cm}^2$) in the growth of AlSb on Si(001). The IMF-based nucleation has enabled optically pumped edge emitters and vertical cavity surface emitting lasers along with superluminescent light emitting diodes.[7] However, the presence of antiphase domains (APDs) has deterred the demonstration of electrically injected lasers on Si (001).

The APD formation in the growth of AlSb on Si (001) is an inherent issue with the growth of polar on nonpolar semiconductors due to a misalignment in group III and group V sublattices at surface steps.[9,10] In the absence of step-free Si(001) substrates, the established method to suppress APD formation uses miscut Si(001) substrates.[11–13] Silicon substrates with 2.5°–5° miscut are typically characterized by a double atomic step height[14] that facilitates registration of the III and V sublattices on the (001) plane thus suppressing APD formation. In the past, high quality III-V material on Si has been produced using the APD annihilation or suppression combined with a strain-relief and defect filtering mechanism, usually a thick buffer layer.[15] These previously reported methods require a two-step growth process initiated at a rather low temperature to enable 60° dislocation formation followed by normal growth temperatures for metamorphic and bulk layer growth. Lattice-matched bulk GaAs epitaxy on miscut Ge has also been demonstrated to produce very low defect and low APD density.[16]

In this paper, we report the growth of III-Sb based epitaxial layers on 5° miscut Si, which simultaneously demonstrates very low defect density ($\sim 7\times10^5/\text{cm}^2$) and very low APD density ($<10^3/\text{cm}^2$). We have already fabricated electrically injected lasers at 1.55 μm on 5° miscut Si (001) operating at 77K through the use of this growth mode, the details of which have been discussed elsewhere.[17] Both the process of strain relief using the IMF array and APD suppression on the miscut substrate occurs at the heterointerface and is described in the following paragraphs. Material parameters are analyzed using plan-view and cross-sectional transmission electron microscope (TEM) images.

The samples used in this interfacial analysis are grown on a V80H molecular beam epitaxy reactor. The IMF formation and required growth conditions on miscut Si is very similar to the IMF on Si (001) described in detail elsewhere.[18] Prior to growth, the Si substrate surface is hydrogen passivated by immersing the wafer in a HF solution bath. Heating the substrate to 500 °C in vacuum removes the loosely bonded hydrogen. A thermal cycle at 800 °C ensures the removal of the oxide remnants. The substrate temperature is reduced and stabilized at 510 °C followed by ~25 s Al soak and then 15 s soak in an Sb overpressure. Following the soak, the AlSb growth is initiated without any changes in the growth temperature resulting in a smoothing of the surface with continued deposition.

Figures 1(a)–1(c) show cross-sectional TEM images of the AlSb/Si interface with the Si substrate having a 5° miscut toward the [110]. Figure 1(a) features a (220) two-beam bright-field low-resolution image, with the bulk AlSb appearing to be free of APDs. Diffraction contrast mainly reflects the long-range strain field in the sample. This image shows a sequence of dark and white bands along the entire interface. In the high-resolution TEM (HRTEM) image of Fig. 1(b),

[a)]Electronic mail: huangsh@unm.edu.

 © 2008 American Institute of Physics

Downloaded 21 Aug 2008 to 129.24.37.97. Redistribution subject to AIP license or copyright; see http://apl.aip.org/apl/copyright.jsp

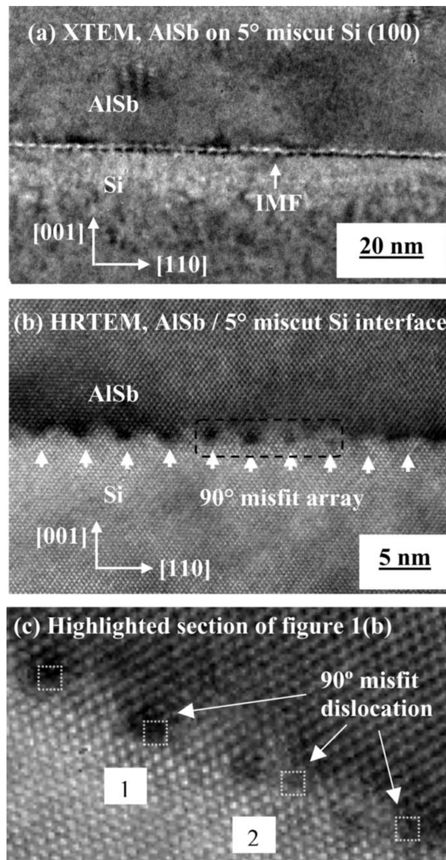

FIG. 1. Cross-sectional TEM images of AlSb grown on 5° miscut Si (001) substrate under (a) low-resolution, (b) high-resolution conditions, and (c) highlighted section of (b), featuring the periodic IMF array.

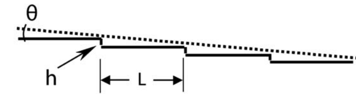

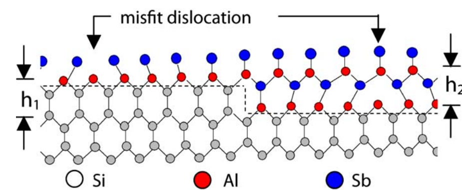

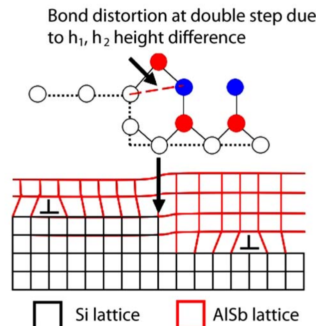

FIG. 2. (Color online) Series of schematics to elucidate atomic arrangement and resulting strain involved in AlSb on miscut Si. Part (a) shows the step geometry on a 5° miscut Si substrate. Part (b) shows a "ball and stick" schematic of Al, Sb, and Si sublattices. Part (c) indicates sources of strain at the step edge due to the h_1, h_2 mismatch.

the lomer dislocation array that constitutes the IMF can be clearly seen. While the strain fields caused by bonds bending around the lomer dislocation are usually the source of the dark and light bands at the misfit dislocation array interfaces,[19] in this case there is no conclusive correlation between the periodic contrast and the location of the misfit dislocation. To investigate this issue further a magnified view of this interface is presented in Fig. 1(c), where the atomic structure becomes clearer. This image shows us that apart from the IMF there is a secondary contrast generating mechanism at the AlSb/Si interface and this is attributed to the presence of periodic steps in the miscut Si substrate. This is evidenced from the fact that moving from left to right along the [110] direction each misfit dislocation lies two Si atomic steps beneath the previous one indicating the presence of double steps in the Si substrate. Furthermore, misfit dislocation labeled "1" is adjacent to a high strain region, while misfit dislocation "2" lies in a relatively low-strain region. We therefore conclude that the dark regions are perhaps associated with the step edge and that the misfit dislocations are randomly placed with respect to the step edges. Burger's circuit theory performed on this image shows that the Burger's vector, i.e., $(a/2)[110]$, lies along the interface and identifies these misfit as 90° pure edge type. The misfit separation, S, is measured to be ~ 3.46 nm and corresponds to exactly eight AlSb lattice sites grown on nine Si lattice sites. This is highly consistent with high quality IMF interfaces that we have realized on Si (100) non-miscut substrates.[18]

In Fig. 2(a), the step length L is defined as $L=h \cot \theta$ where h is the step height and θ is the miscut angle. The double atomic steps on 5° miscut Si (001) yields $h=2.72$ Å, thus $L=h \cot \theta = 2.72 \cot 5° = 31.09$ Å. This value is fairly well matched to IMF spacing S and results in a single IMF per step. At the double-step step edge, where the Al and Sb layers growing on the upper and lower steps are closely registered, a significant strain is generated. Although Al–Si bond is larger (2.45 Å) than Si–Si (2.17 Å), in $AlSi_2$ cluster the Al–Si bond shrinks significantly and it becomes almost equal to that of Si–Si bonds (2.36 for Al–Si and 2.38 for Si–Si).[20] The Al atom substitutes one of the Si atoms from the host Si cluster, only causing a small local distortion. Therefore, the source of the strain is the height differential in the Si double step h_1 and the two-atom-layer height of AlSb lattice h_2 in the [001] direction, as shown in Fig. 2(b). Using the following values of $h_1=2.72$ Å and $h_2=3.06$ Å, we calculate a mismatch of 12.5% along the [001] direction. This causes the AlSb layer growing on the lower step to be compressed along the [001] direction to facilitate registration. The effect of this strain at the Si double step is depicted in Fig. 2(c), which shows a cubic approximation of the AlSb/Si lattice. The illustration shows a significant strain at the double step and also strain around the misfit dislocation and supports the strain seen in the TEMs of Figs. 1(a)–1(c). Since the miscut is 5° toward the [110] direction, we expect that this effect is only along the [110] direction and is not repeated along the [1−10] direction. However, the same regular IMF array as that of AlSb/Si (001) interface[18] has also been observed along [1−10] direction (not shown), which shows that there is a two-dimensional (2D) array of

Downloaded 21 Aug 2008 to 129.24.37.97. Redistribution subject to AIP license or copyright; see http://apl.aip.org/apl/copyright.jsp

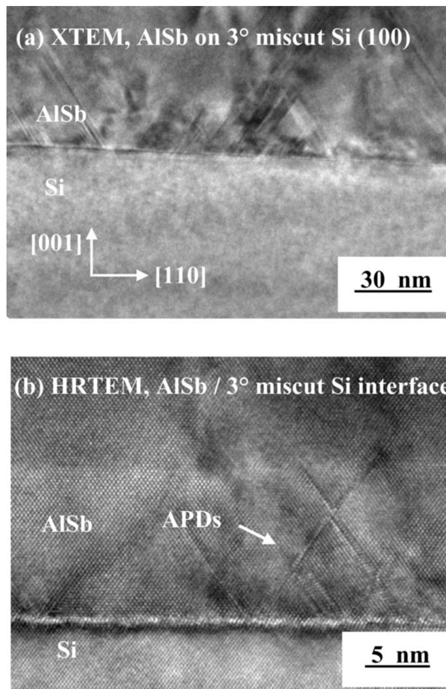

FIG. 3. Cross-sectional TEM image of AlSb grown on 3° miscut Si (001) substrate under (a) low-resolution and (b) high-resolution conditions featuring defects and APDs.

pure 90° edge dislocation confined to this interface.

The double step height, h, is critical for achieving APD suppression on the miscut Si substrate. The importance of L relative to S, for high quality IMF formation, is suggested by a comparison of AlSb grown on 3°, 5°, and 6° miscut substrates, respectively, grown under similar conditions. Figure 3(a) shows the AlSb bulk on 3° miscut Si (001) substrate along the [110] direction. The APDs and defect density are $>10^7/\text{cm}^2$ as measured using atomic force microscope and plan-view TEMs, respectively. Figure 3(b) shows the corresponding IMFs using HRTEM image. For a 3° miscut, the step height may be a single step, double step, or a mixture. For a single step, $h=1.35$ Å, the step length, $L=h\cot\theta=1.35\cot 3°=25.72$ Å$<S$. For a double step, $h=2.72$ Å, the step length, $L=h\cot\theta=2.72\cot 3°=51.90$ Å$>S$. Similarly, the AlSb bulk on 6° miscut Si (001) substrate produces rather large defect density (not shown here for brevity sake). Its step length L is also far away from IMF spacing S. While we cannot substantiate any required relations between L and S, a step length L that is significantly shorter or longer than the IMF spacing will increase the number of interaction points between the step edge and the 90° misfit which may initiate other misfit formation.

Sample quality analysis by TEM images verifies dislocation and APD density in bulk GaSb grown on the AlSb/Si IMF. Figure 4 shows low magnification XTEM image, indicating that the GaSb epilayer appears to be free of defects and APDs. Based on scanning several wafer surfaces, we estimate the defect density to be $\sim 7\times 10^5$ defects/cm^2 and the average APD density in the wafer surface is $<10^3/\text{cm}^2$.

In conclusion, we have demonstrated and characterized the simultaneous APD suppression and IMF formation in the growth of AlSb on 5° miscut Si (001). The step length of the

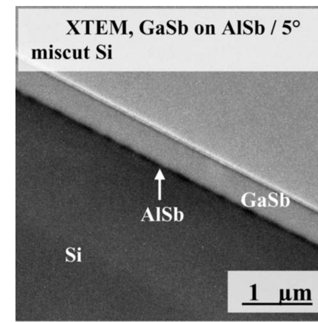

FIG. 4. Sample quality analysis of GaSb bulk nucleated via an AlSb IMF on 5° miscut Si by cross-sectional TEM image.

5° miscut substrate is shown to be fairly well matched to the IMF spacing and allows the formation of a single 90° misfit dislocation per step thus facilitating the formation of the IMF. The AlSb bulk with low dislocation density, strain-relieved properties generated by the growth conditions can provide a promising technology for the monolithic integration of III-V devices on Si substrate.

[1]K. K. Linder, J. Phillips, O. Qasaimeh, X. F. Liu, S. Krishna, P. Bhattacharya, and J. C. Jiang, Appl. Phys. Lett. **74**, 1355 (1999).
[2]D. G. Deppe, N. Holonyak, Jr., K. C. Hsieh, D. W. Nam, and W. E. Plano, Appl. Phys. Lett. **52**, 1812 (1988).
[3]O. Kwon, J. J. Boeckl, M. L. Lee, A. J. Pitera, E. A. Fitzgerald, and S. A. Ringel, J. Appl. Phys. **100**, 013103 (2006).
[4]M. E. Groenert, C. W. Leitz, A. J. Pitera, V. Yang, H. Lee, R. J. Ram, and E. A. Fitzgerald, J. Appl. Phys. **93**, 362 (2003).
[5]I. Hwang, C. Lee, J.-E. Kim, and H. Y. Park, Phys. Rev. B **51**, 7894 (1995).
[6]S. H. Huang, G. Balakrishnan, A. Khoshakhlagh, A. Jallipalli, L. R. Dawson, and D. L. Huffaker, Appl. Phys. Lett. **88**, 131911 (2006).
[7]G. Balakrishnan, S. H. Huang, A. Khoshakhlagh, A. Jallipalli, P. Rotella, A. Amtout, S. Krishna, C. P. Haines, L. R. Dawson, and D. L. Huffaker, Electron. Lett. **42**, 6 (2006).
[8]S. H. Huang, G. Balakrishnan, M. Mehta, A. Khoshakhlagh, L. R. Dawson, D. L. Huffaker, and P. Li, Appl. Phys. Lett. **90**, 161902 (2007).
[9]*Heteroepitaxy on Silicon*, edited by J. C. C. Fan and J. M. Poate (Materials Research Society, Pittsburgh, PA, 1986), Vol. 67.
[10]*Heteroepitaxy on Silicon: Fundamentals, Structure and Devices*, edited by H. K. Choi, R. Hull, H. Ishiwara, and R. J. Nemanich (Materials Research Society, Pittsburgh, PA, 1988), Vol. 116.
[11]K. Adomi, S. Strite, H. Morkoc, Y. Nakamura, and N. Otsuka, J. Appl. Phys. **69**, 220 (1991).
[12]C. L. Andre, J. A. Carlin, J. J. Boeckl, D. M. Wilt, M. A. Smith, A. J. Pitera, M. L. Lee, E. A. Fitzgerald, and S. A. Ringel, IEEE Trans. Electron Devices **52**, 1055 (2005).
[13]R. M. Sieg, S. A. Ringel, S. M. Ting, S. B. Samavedam, M. Currie, T. Langdo, and E. A. Fitzgerald, J. Vac. Sci. Technol. B **16**, 1471 (1998).
[14]L. Barbier, A. Khater, B. Salanon, and J. Lapujoulade, Phys. Rev. B **43**, 14730 (1991).
[15]J. Yang, Z. Mi, and P. Bhattacharya, J. Lightwave Technol. **25**, 1826 (2007).
[16]H. Tanoto, S. F. Yoon, W. K. Loke, E. A. Fitzgerald, C. Dohrman, B. Narayanan, and C. H. Tung, *MRS Symposia Proceedings* No. 891 (Materials Research Society, Pittsburgh, 2006), p. EE03-17.1.
[17]A. Jallipalli, M. N. Kutty, G. Balakrishnan, J. Tatebayashi, N. Nuntawong, S. H. Huang, L. R. Dawson, and D. L. Huffaker, Electron. Lett. **43**, 1198 (2007).
[18]G. Balakrishnan, A. Jallipalli, S. H. Huang, A. Khoshakhlagh, P. Rotella, A. Amtout, S. Krishna, C. P. Haines, L. R. Dawson, and D. L. Huffaker, IEEE J. Sel. Top. Quantum Electron. **12**, 1636 (2006).
[19]M. De Giorgi, A. Taurino, A. Passaseo, M. Catalano, and R. Cingolani, Phys. Rev. B **63**, 245302 (2001).
[20]S. Nigam, C. Majumder, and S. K. Skulshreshtha, J. Chem. Phys. **121**, 7756 (2004).

Downloaded 21 Aug 2008 to 129.24.37.97. Redistribution subject to AIP license or copyright; see http://apl.aip.org/apl/copyright.jsp